Supplemental Material for Pixel Screening based Intermediate Correction for Blind Deblurring

Meina Zhang[1] Yingying Fang[2] Guoxi Ni[1*] Tieyong Zeng[3*]
[1]Institute of Applied Physics and Computational Mathematics, Beijing, China
[2] Imperial College London, London, United Kingdom
[3]The Chinese University of Hong Kong, Shatin, Hong Kong
mnzhang01@gmail.com, y.fang@imperial.ac.uk, gxni@iapcm.ac.cn, zeng@math.cuhk.edu.hk

1. Overview

In this material, we provide more experimental results on the challenging cases to further prove the effectiveness and leading performance of the proposed method. The supplementary material is organized as follows. In Sec. 2, we present more visual comparisons of images with large kernels from Lai *et al*.'s dataset [5]. In Sec. 3, we give more comparisons on real-world images. In Sec. 4, we illustrate more results of the proposed method with and without the intermediate correction step to verify the effectiveness of the proposed pixel screening strategy. In Sec. 5, we further extend the proposed strategy to other state-of-the-art methods to prove its flexibility and effectiveness.

2. Lai *et al*.'s dataset

In Fig. 1 and Fig. 2, we compare the proposed model with Xu *et al*. [11], Michaeli *et al*. [7], Dong *et al*. [4], Chen *et al*. [1], Chen-sat [3], Liu *et al*. [6]. As Fig. 1 shows, the proposed method gets the most accurate kernel, with which the final deblurred image contains minimal artifacts. In Fig. 2, the estimated kernel by our method is closest to the ground-truth kernel and the deblurred image also reaches the best visual performance .

3. Real-world images

In this part, we present more results of images captured in the real scenes from Fig. 3 to Fig. 7. Especially, we select images of low-illumination, which are particularly challenging for blind deblurring. We compare our method to the state-of-the-art methods [1,3,4,6,8–10]. From Fig. 3 to Fig. 7, we can see all other methods fail to derive the blurring kernels in one case or two cases and converge to the input kernel as a dot while our method is stable to derive the blurring kernel to deblur the final sharp images. Compared with those algorithms specifically designed for saturated images [3, 4, 9], our method is also comparable and even shows better results.

4. With and without intermediate correction

As our method without the pixel screening strategy will reduce to [6], this section emphasizes the comparison of the proposed method with [6] from Fig. 1 to Fig. 8. As we can see, the method of [6] is vulnerable in the cases with saturated points and hardly derives the accurate kernels. In contrast,applying the image correction to [6] can greatly improve its performance in these cases. Particularly, a comparison of the methods with and without the intermediate correction is presented in Fig. 8.

5. Extension to other methods

We apply the pixel screening map and the intermediate image correction step to other blind deblurring methods [1–4, 9, 10] which are divided into three classes. As the public codes of [3,4,9] are encrypted, we reproduce them with the performance as the public and then apply our method on them to prove its effectiveness.

Prior based methods. The proposed post-processing strategy is applied to the methods [1] and [10]. The comparisons with and without image correction step are given in Fig. 9 Fig. 10. The proposed method makes up for their inability to handle the saturated images.

Edge selection based methods. We apply the proposed correction map to the intermediate image of [9] before their edge selection step. As Fig. 11 shows, the method with intermediate correction derives more accurate kernel which removes the blur in the final latent image.

Outlier processing methods. For the outliers handling methods [2–4], we remove the undesirable pixels in their intermediate images before their kernel estimation step. As Fig. 12, Fig. 13, Fig. 14 show, we improved their performance on processing the saturated images.

*Corresponding authors

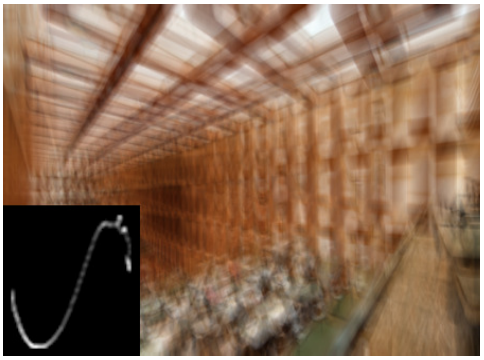

(a) Blurry image

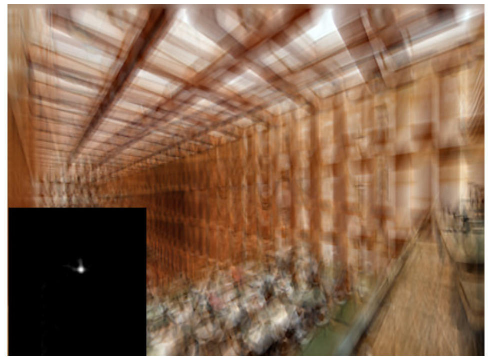

(b) Michaeli *et al*. [7]

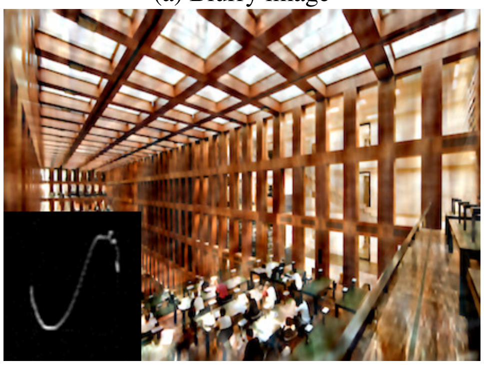

(c) Xu *et al*. [11]

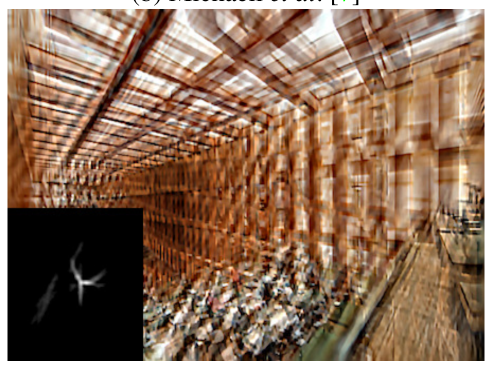

(d) Chen *et al*. [1]

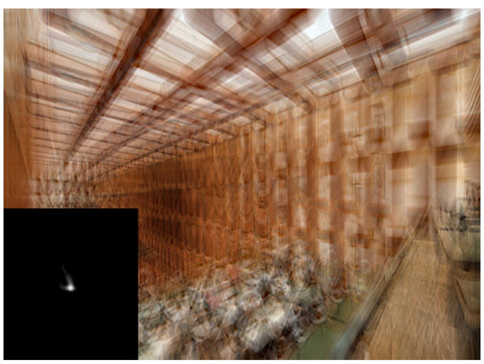

(e) Dong *et al*. [4]

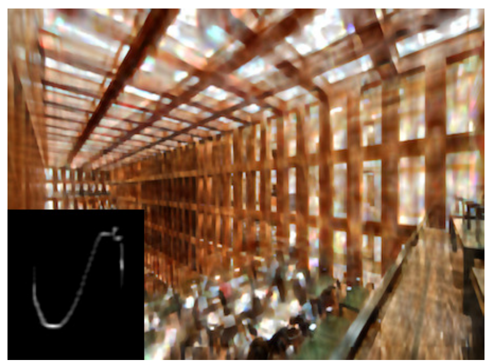

(f) Chen-sat [3]

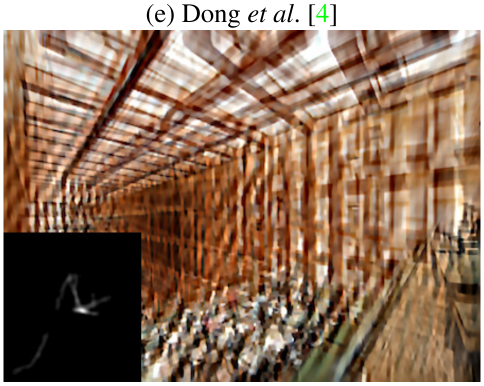

(g) Liu *et al*. [6]

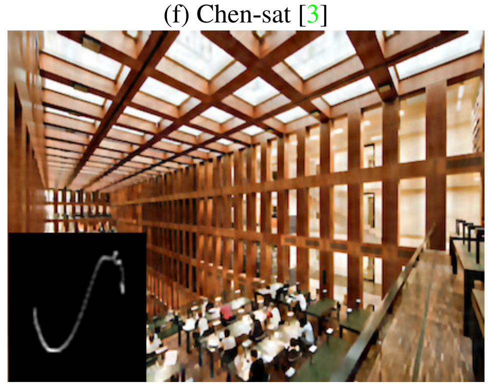

(h) Ours

Figure 1. The comparison of an example from Lai's dataset *et al*. [5] with large blur. In the left bottom corner list the kernels estimated by different methods except the one in (a) is the exact blurring kernel applied to synthesize the blurry image. Our method is effective in estimating the large blur kernels, comparing to other state-of-the-art methods. The final deblurred image with our kernel contains least artifacts.

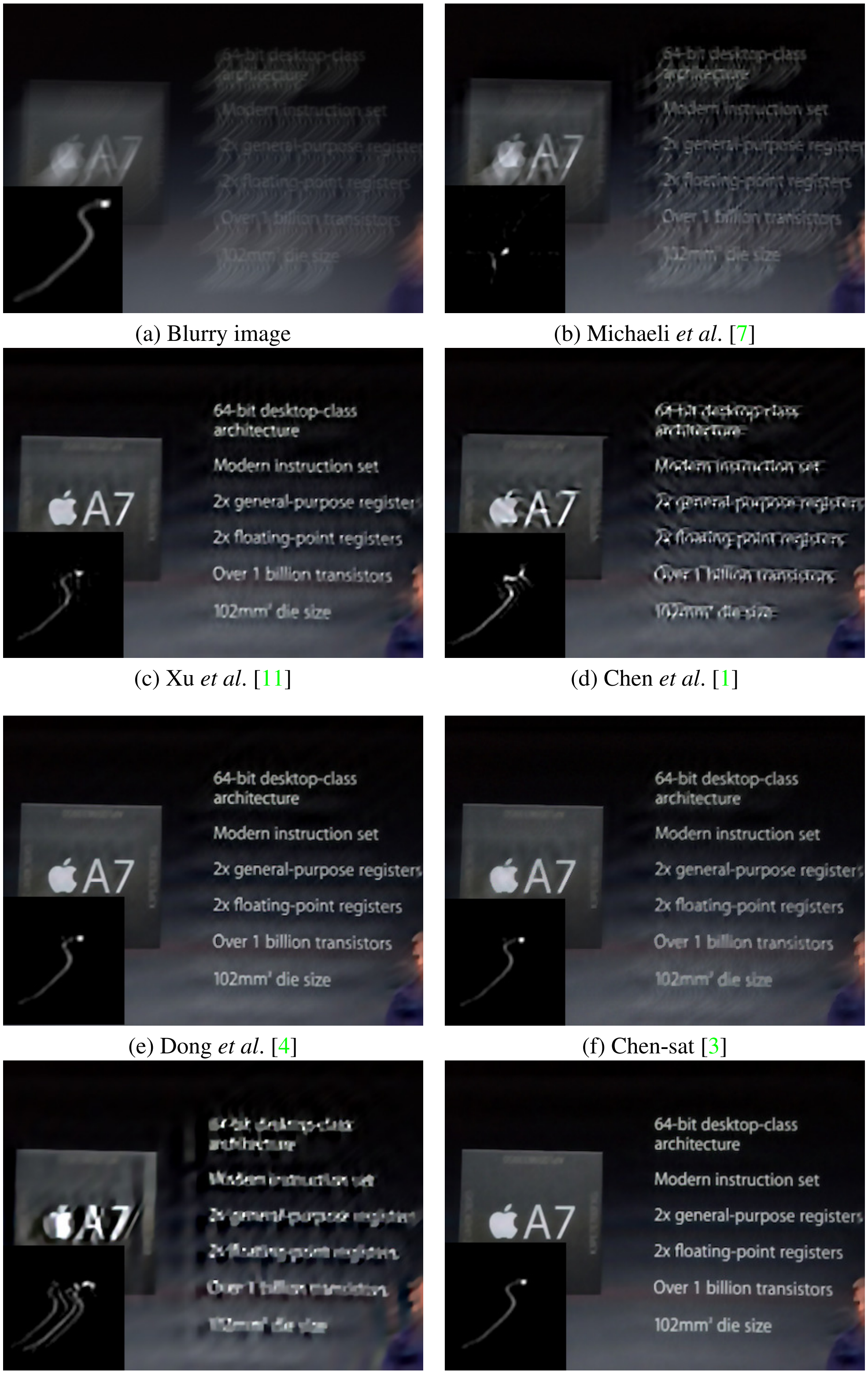

(a) Blurry image (b) Michaeli *et al*. [7]

(c) Xu *et al*. [11] (d) Chen *et al*. [1]

(e) Dong *et al*. [4] (f) Chen-sat [3]

(g) Liu *et al*. [6] (h) Ours

Figure 2. The comparison of an example from Lai's dataset *et al*. [5] with large blur. In the left bottom corner list the kernels estimated by different methods except the one in (a) is the exact blurring kernel applied to synthesize the blurry image. Our method is effective in estimating the large blur kernels, comparing to other state-of-the-art methods. The final deblurred image with our estimated kernel reaches the sharpest visual quality with least ringing artifacts.

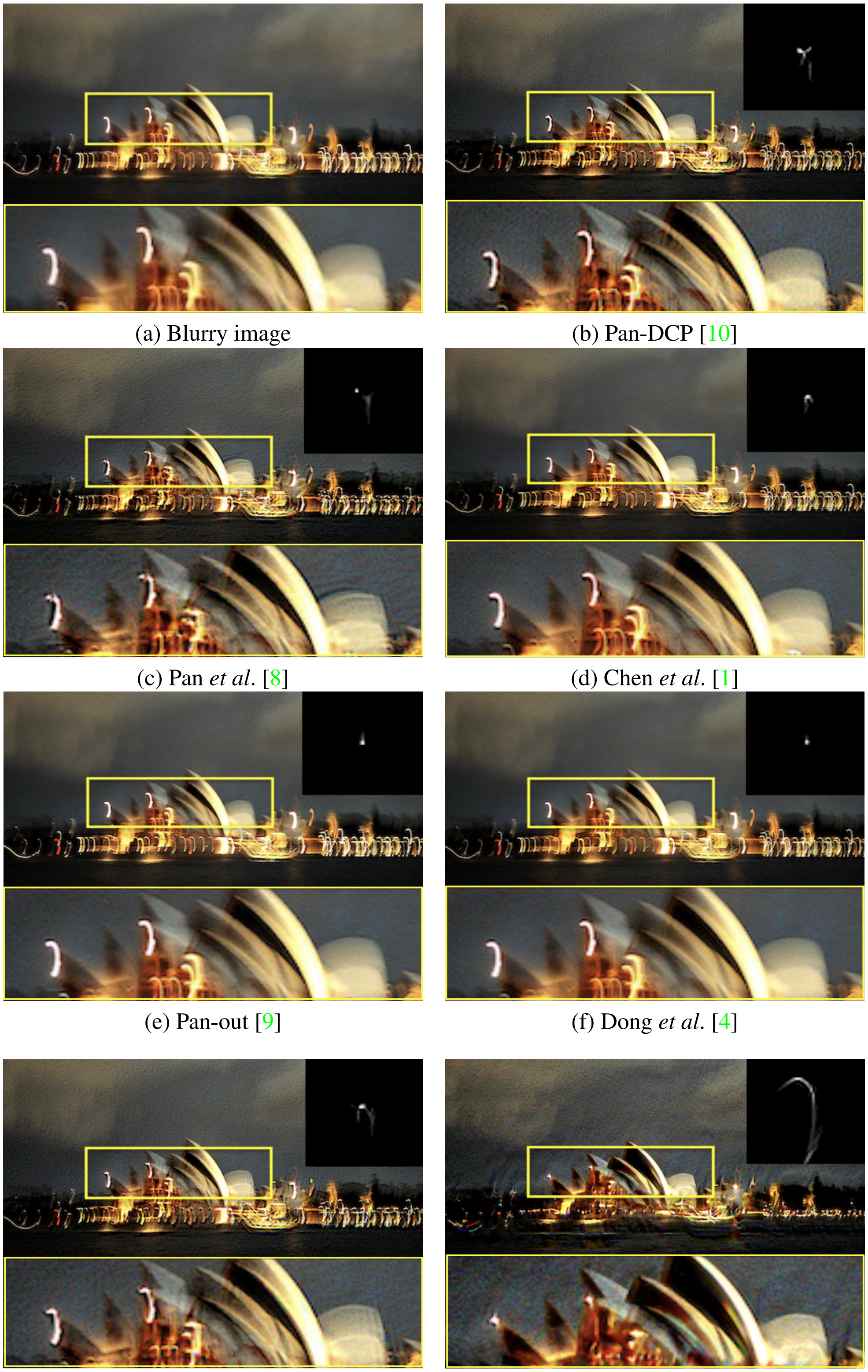

(a) Blurry image
(b) Pan-DCP [10]
(c) Pan *et al*. [8]
(d) Chen *et al*. [1]
(e) Pan-out [9]
(f) Dong *et al*. [4]
(g) Liu *et al*. [6]
(h) Ours

Figure 3. Visual comparison of a low-light image, we can see from zoomed area that our method effectively eliminates the light streaks caused by blur.

(a) Blurry image (b) Pan-DCP [10]

(c) Pan *et al*. [8] (d) Chen *et al*. [1]

(e) Dong *et al*. [4] (f) Chen-sat [3]

(g) Liu *et al*. [6] (h) Ours

Figure 4. Visual comparison of a low-illumination image captured in the real scene, our method recovers the final image contains minimal artifacts and removes blur from the saturated area.

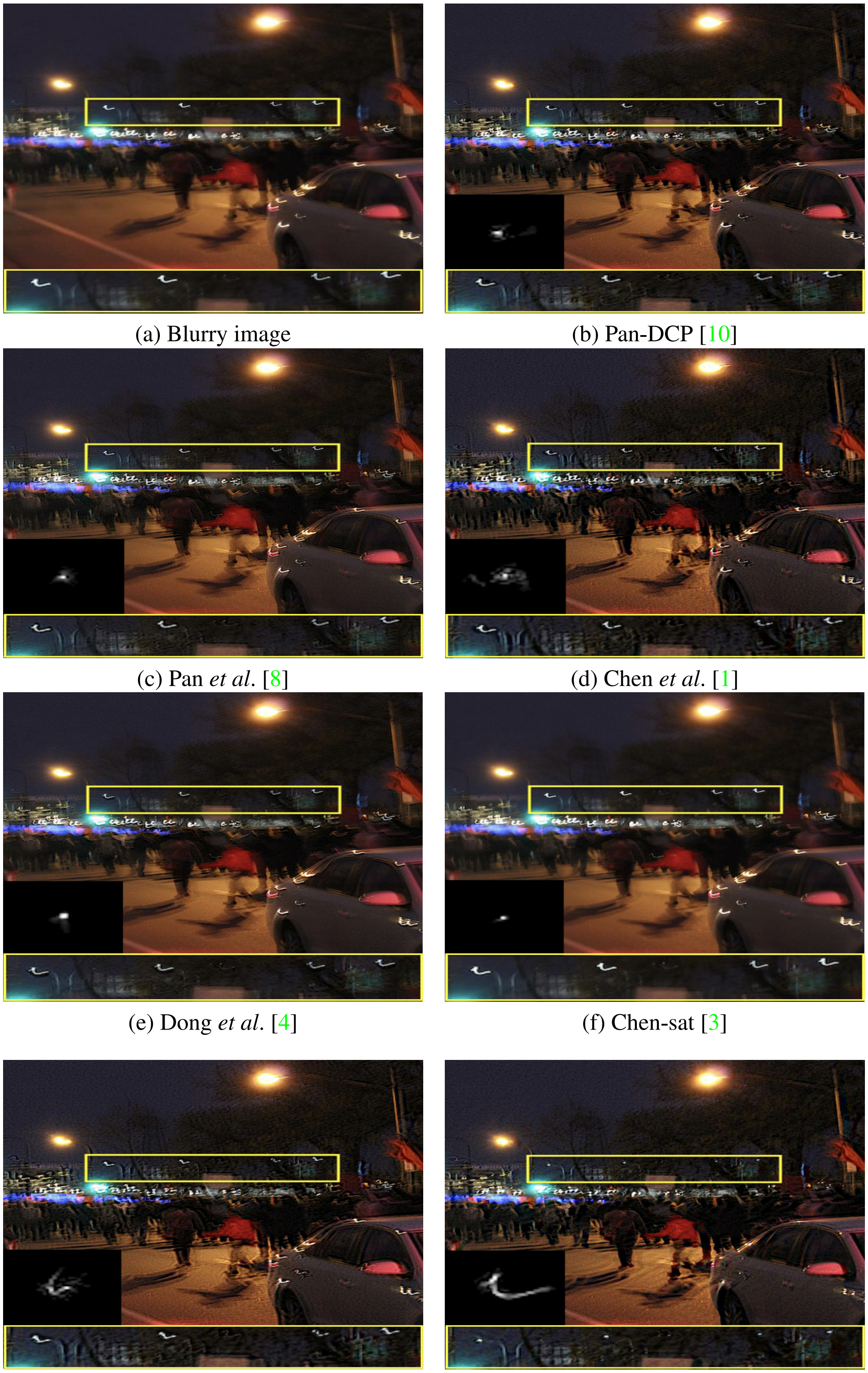

(a) Blurry image
(b) Pan-DCP [10]
(c) Pan *et al*. [8]
(d) Chen *et al*. [1]
(e) Dong *et al*. [4]
(f) Chen-sat [3]
(g) Liu *et al*. [6]
(h) Ours

Figure 5. Visual comparison of estimated kernel and deblurred results of a low-illumination image, our method explicitly removes the blur in the saturated area.

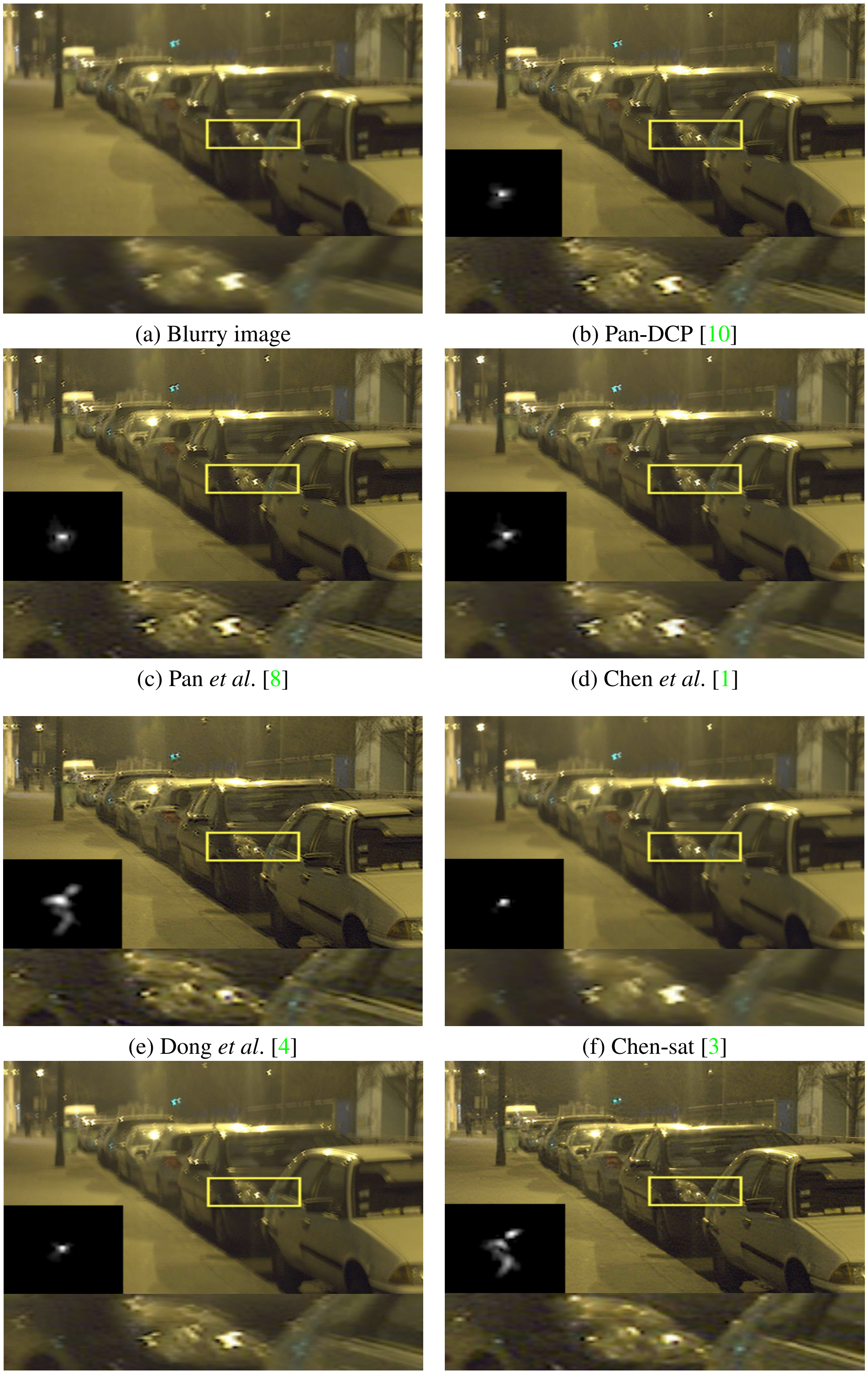

(a) Blurry image (b) Pan-DCP [10]
(c) Pan *et al.* [8] (d) Chen *et al.* [1]
(e) Dong *et al.* [4] (f) Chen-sat [3]
(g) Liu *et al.* [6] (h) Ours

Figure 6. Deblurred results of a low-light image, our method removes the blur in the saturated pixels.

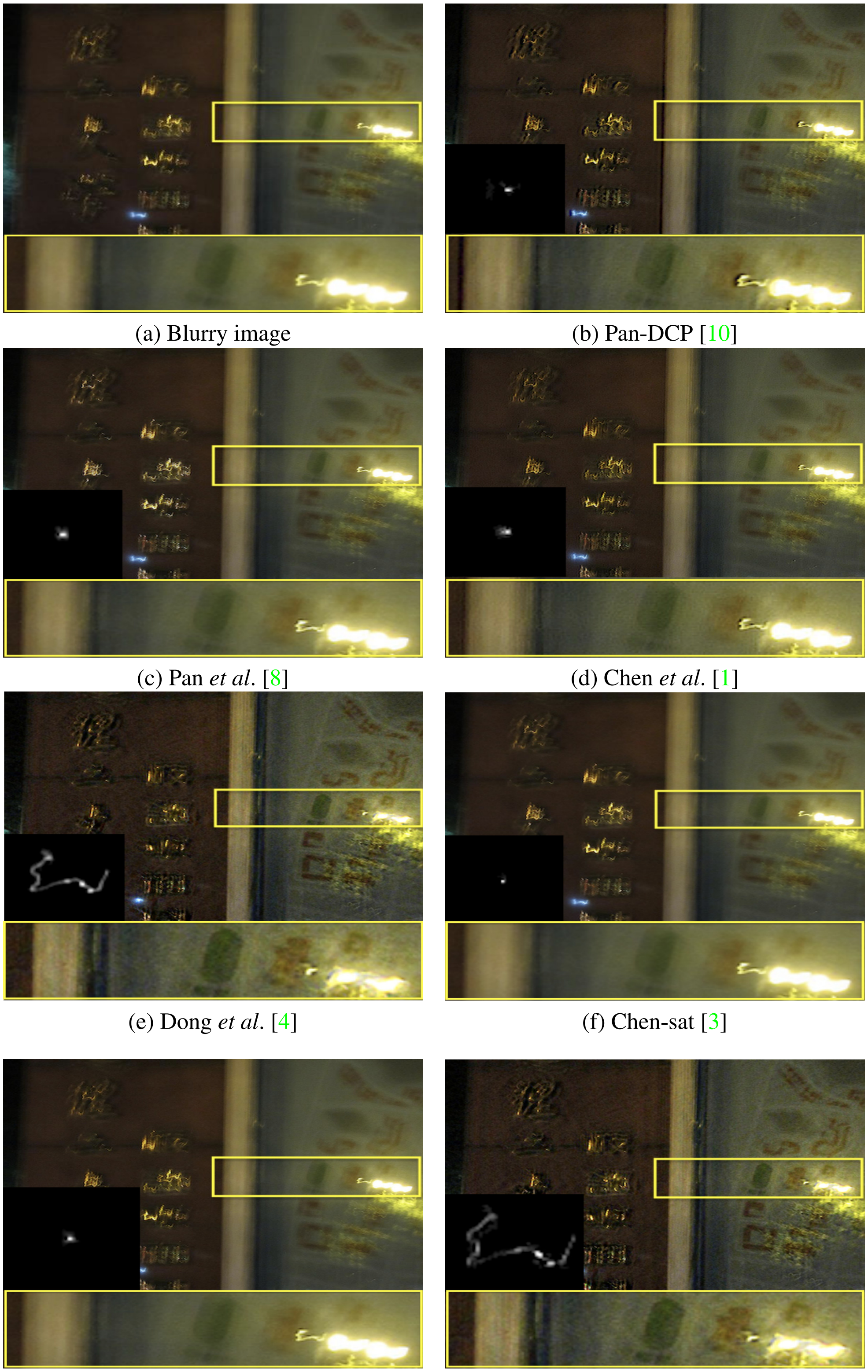

(a) Blurry image
(b) Pan-DCP [10]
(c) Pan *et al.* [8]
(d) Chen *et al.* [1]
(e) Dong *et al.* [4]
(f) Chen-sat [3]
(g) Liu *et al.* [6]
(h) Ours

Figure 7. Deblurred results of a saturated image, the proposed method is comparable with state-of-the-arts.

(a) Blurry image (b) Liu *et al*. [6] (c) Ours (d) Liu *et al*. [6] (e) Ours

Figure 8. Visual comparison of deblurred results before and after intermediate correction, where (b) and (c) are the intermediate latent images of final result (d) and (e). Affected by the saturated pixels, the method of Liu [6] fails in estimating the blur kernel with any shape. In shape contrast to it, our method recovers accurate blur kernels and high quality deblurred images after intermediate correction that reduce those disadvantageous pixels. The images are best compared by zooming in.

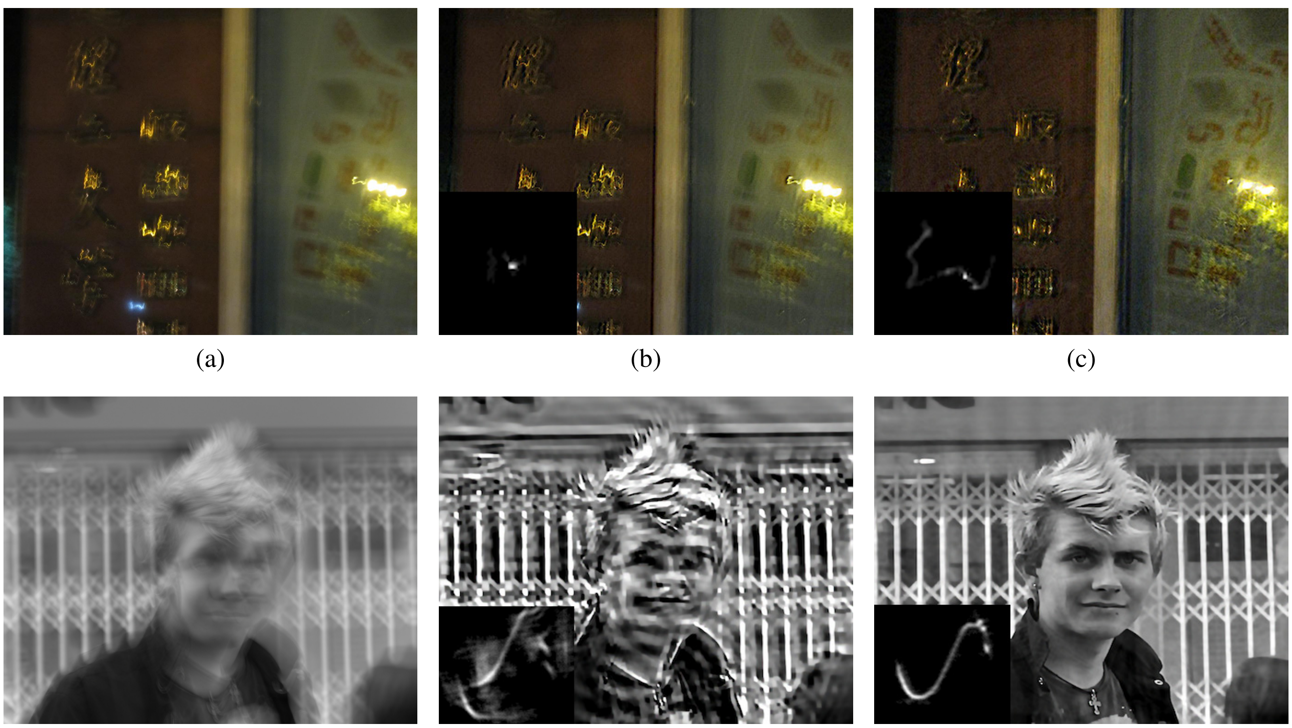

(a) (b) (c)

(a) (b) (c)

Figure 9. Comparisons of [10] with and without our method, (a) the blurry images, (b) results of [10], (c) results of [10] with our correction.

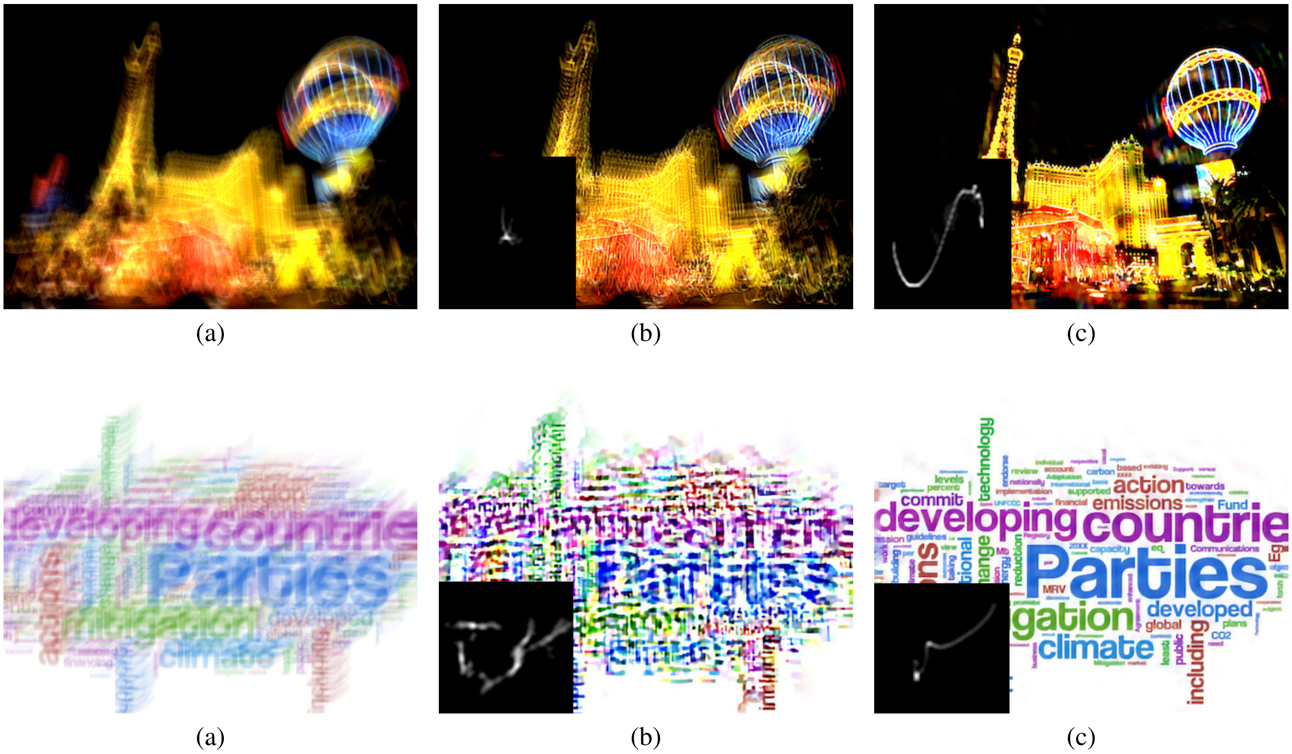

Figure 10. Comparisons of [1] with and without our method. (a): the blurry images, (b): results of [1], (c): results of [1] with our correction. Please zoom in for best visualization.

Figure 11. Comparisons of [9] with and without our method. (a): the blurry images, (b): results using [9], (c): reproduced results, (d): results using our strategy. Please zoom in for best visualization.

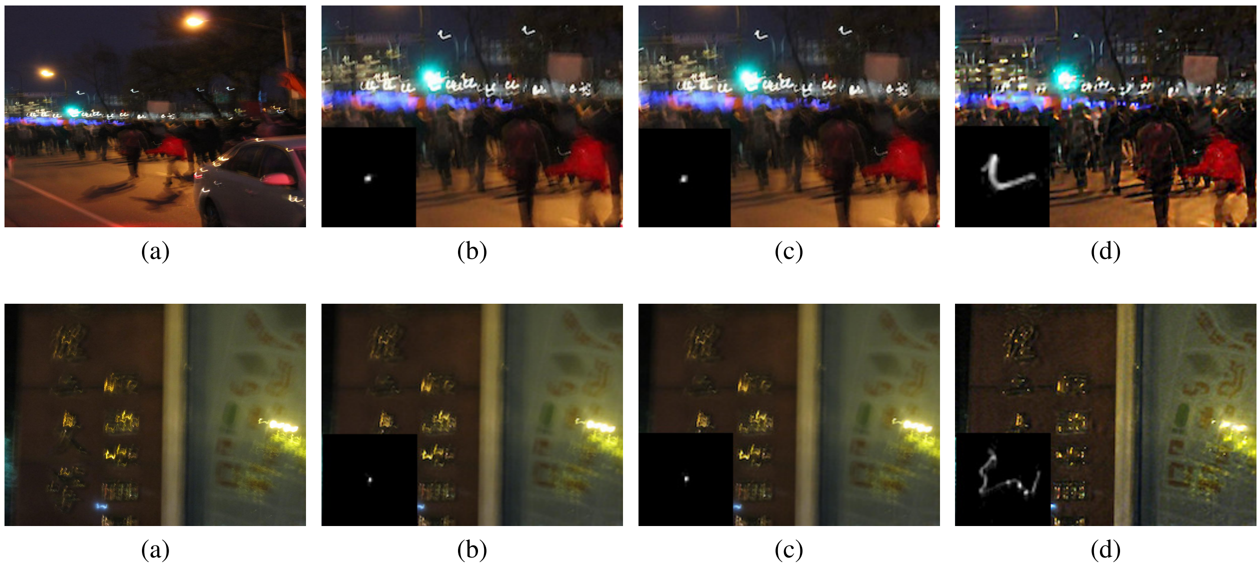

Figure 12. Comparisons of [3] with and without our method. (a): the blurry images, (b): results using [3], (c): reproduce results, (d): Results using our strategy. Please zoom in for best visualization.

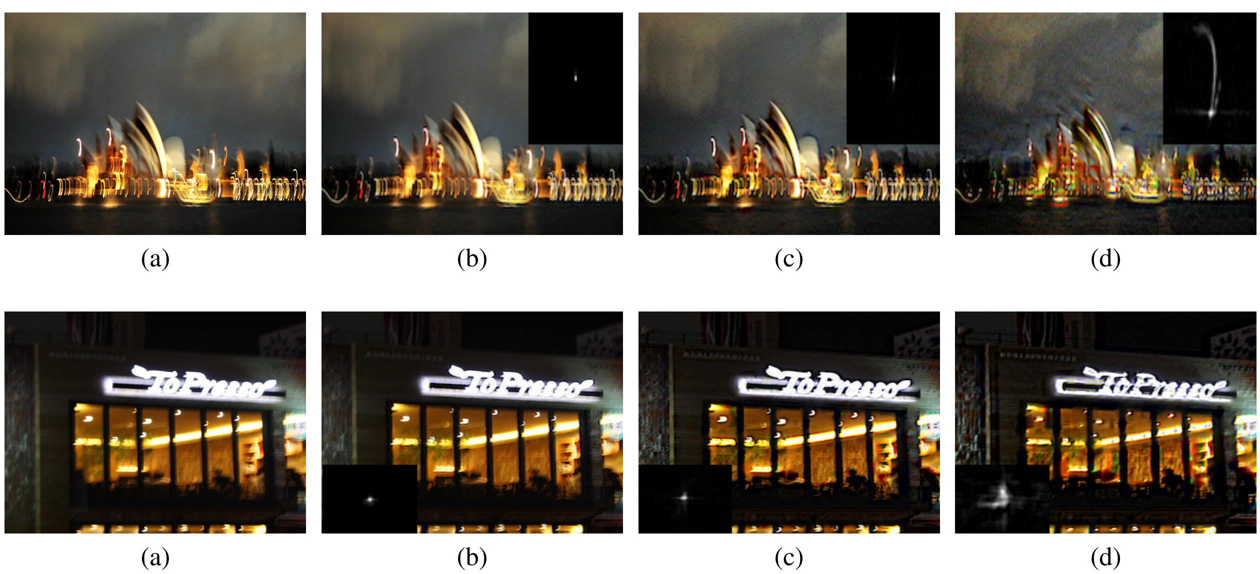

Figure 13. Comparisons of [4] with and without our method. (a): the blurry images, (b): results using [4], (c): reproduce results, (d): results using our strategy. Please zoom in for best visualization.

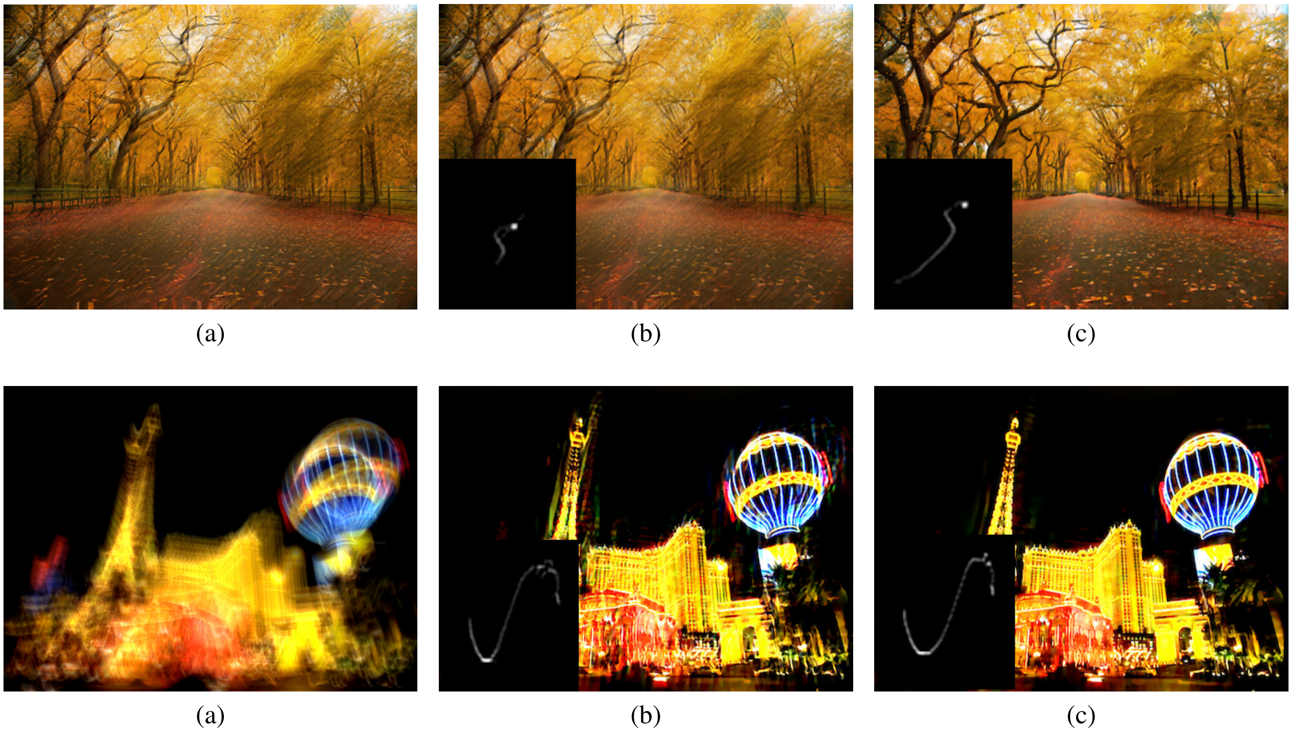

Figure 14. Comparisons of [2] with and without our method. (a): the blurry images, (b): results using [2], (c): results using our strategy. Please zoom in for best visualization.

References

[1] L. Chen, F. Fang, T. Wang, and G. Zhang. Blind image deblurring with local maximum gradient prior. *CVPR*, pages 1742–1750, 2019. 1, 2, 3, 4, 5, 6, 7, 8, 10

[2] L. Chen, F. Fang, J. Zhang, J. Liu, and G. Zhang. OID: Outlier identifying and discarding in blind image deblurring. *ECCV*, pages 598–613, 2020. 1, 12

[3] L. Chen, J. Zhang, S. Lin, F. Fang, and J. Ren. Blind deblurring for saturated images. *CVPR*, pages 6308–6316, June 2021. 1, 2, 3, 5, 6, 7, 8, 11

[4] J. Dong, J. Pan, Z. Su, and M. Yang. Blind image deblurring with outlier handling. *ICCV*, pages 2497–2505, 2017. 1, 2, 3, 4, 5, 6, 7, 8, 11

[5] W. S. Lai, J. B. Huang, Z. Hu, N. Ahuja, and M. H. Yang. A comparative study for single image blind deblurring. *CVPR*, pages 1701–1709, 2016. 1, 2, 3

[6] J. Liu, M. Yan, and T. Zeng. Surface-aware blind image deblurring. *IEEE TPAMI*, 43(3):1041–1055, 2021. 1, 2, 3, 4, 5, 6, 7, 8, 9

[7] T. Michaeli and M. Irani. Blind deblurring using internal patch recurrence. *ECCV*, pages 783–798, 2014. 1, 2, 3

[8] J. Pan, Z. Hu, Z. Su, and M. H. Yang. L0-regularized intensity and gradient prior for deblurring text images and beyond. *IEEE TPAMI*, 39(2):342–355, 2017. 1, 4, 5, 6, 7, 8

[9] J. Pan, Z. Lin, Z. Su, and M. Yang. Robust kernel estimation with outliers handling for image deblurring. *CVPR*, pages 2800–2808, 2016. 1, 4, 10

[10] J. Pan, D. Sun, H. Pfister, and M. H. Yang. Blind image deblurring using dark channel prior. *CVPR*, page 1628–1636, 2016. 1, 4, 5, 6, 7, 8, 9

[11] L. Xu, S. Zheng, and J. Jia. Unnatural L0 sparse representation for natural image deblurring. *CVPR*, pages 1107–1114, 2013. 1, 2, 3